Appl. Phys. A 71, 101–104 (2000) / Digital Object Identifier (DOI) 10.1007/s003390000544

Applied Physics A
Materials
Science & Processing

Rapid communication

Epitaxial growth of non-c-oriented ferroelectric $SrBi_2Ta_2O_9$ thin films on Si(100) substrates

H.N. Lee, S. Senz, A. Visinoiu, A. Pignolet, D. Hesse, U. Gösele

Max-Planck-Institut für Mikrostrukturphysik, Weinberg 2, 06120 Halle/Saale, Germany
(Fax: +49-345/5511-223, E-mail: hnlee@mpi-halle.de)

Received: 5 April 2000/Accepted: 7 April 2000/Published online: 7 June 2000 –

Abstract. Epitaxial $SrBi_2Ta_2O_9$ (SBT) thin films with well-defined (116) orientation have been grown by pulsed laser deposition on Si(100) substrates covered with an yttria-stabilized ZrO_2 (YSZ) buffer layer and an epitaxial layer of electrically conductive $SrRuO_3$. Studies on the in-plane crystallographic relations between $SrRuO_3$ and YSZ revealed a rectangle-on-cube epitaxy with respect to the substrate. X-ray diffraction pole figure measurements revealed well-defined orientation relations, viz. SBT(116)‖$SrRuO_3$(110)‖YSZ(100)‖Si(100), SBT[110]‖$SrRuO_3$[001], and $SrRuO_3$[111]‖YSZ[110]‖Si[110].

PACS: 77.84.-s; 68.55.-a; 81.15.Fg

Numerous investigations of polycrystalline ferroelectric $SrBi_2Ta_2O_9$ (SBT) thin films have been stimulated by a fundamental scientific interest and by prospective technical applications in ferroelectric nonvolatile memories due to the high fatigue endurance of SBT [1]. However, the application of polycrystalline SBT thin films suffers from certain limitations. For instance, it is difficult to obtain ferroelectric properties homogeneous over the different cells of a large capacitor-array when the lateral size of ferroelectric cells drops below 100 nm, corresponding to cell sizes needed for Gigabit memories [2, 3]. Also, the existence of ferroelectric properties and their dependenc on the cell size and material in such small structures (size effect) has been recently addressed [4, 5].

Successful efforts of an epitaxial growth of SBT thin films deposited by pulsed laser deposition (PLD), metalorganic chemical vapor deposition (MOCVD), and rf magnetron sputtering methods, have been reported [6–9]. In all of these works, special single crystalline substrates such as $SrTiO_3$, $LaAlO_3$-Sr_2AlTaO_6, $LaSrAlO_4$, and MgO of various orientations have been used to grow epitaxial c-axis-oriented as well as non-c-axis oriented SBT thin films. It was generally found that c-oriented epitaxial SBT films, i.e. films with their (001) plane parallel to the substrate surface, can be grown on $SrTiO_3$(100) substrates, whereas epitaxial SBT films that have the (116) and (103) plane parallel to the substrate surface, grow on $SrTiO_3$(110) and (111) substrates, respectively. These observations are, however, not of high practical significance for memory devices, because $SrTiO_3$ crystals are not suitable substrates in microelectronics. For a better compatibility with silicon-based microelectronics, epitaxial SBT films should be grown on silicon substrates. To our knowledge, there is no report on the epitaxial growth of non-c-oriented SBT on Si(100) to date. We report here on epitaxial SBT(116) films on Si(100).

The growth of non-c-oriented SBT films is of particular significance because the vector of the spontaneous electrical polarization in SBT is directed along the a-axis [10]. This means that a c-oriented SBT thin film does not have a polarization component along its film normal (perpendicular to the film plane). Such a component is, however, essential, if the SBT film is to be used in a ferroelectric thin-film capacitor with electrodes on the top and bottom film surfaces. This is the very reason why non-c-axis-oriented, epitaxial SBT films on Si(100) are particularly interesting in view of future applications.

Epitaxial $SrRuO_3$ thin films have been found useful as electrodes for ferroelectric capacitors, due to the high thermal and chemical stability of $SrRuO_3$ and because of its good lattice match with $SrTiO_3$ and $Pb(ZrTi)O_3$. $SrRuO_3$ is a pseudocubic perovskite with a slight orthorhombic distortion due to the tilting of the RuO_6 octahedra. High quality epitaxial $SrRuO_3$ films have been successfully deposited on different substrates, such as $SrTiO_3$(100) and $LaAlO_3$(100) and by different methods like off-axis sputtering and PLD [11–13]. Recently, epitaxial (116)- and (103)-oriented SBT thin films grown on $SrRuO_3$ base electrodes deposited on lattice-matched perovskite $SrTiO_3$ substrates have been demonstrated [7, 14–17]. However, these substrates are not used in making integrated devices as mentioned above. In this work, we report the heteroepitaxial growth of SBT(116) thin films on Si(100) substrates by PLD. The key structural component responsible for the epitaxial growth of SBT(116) is a $SrRuO_3$(110) layer on yttria-stabilized ZrO_2 (YSZ)(100)-buffered Si(100).

1 Experimental

PLD was used to deposit SBT and $SrRuO_3$ thin films as well as YSZ using a PLD setup similar to that described previously [9, 18]. Briefly, a KrF excimer laser ($\lambda = 248$ nm), operating at a repetition rate of 5 Hz with an energy density of 2–4 J/cm^2, was used to deposit SBT thin films onto $SrRuO_3$/YSZ/Si(100). The base pressure in the chamber was 5×10^{-8} mbar before raising the substrate temperature. *p*-Si(100) wafers with a resistivity of 1–5 Ω cm were used as substrates. An epitaxial YSZ thin film 75 nm thick was first grown on the Si(100) substrate at a substrate temperature of 800 °C with a flowing O_2 pressure of 1.7×10^{-3} mbar. Details on the epitaxial growth of YSZ on Si had been described previously [19, 20]. The $SrRuO_3$ film with a thickness of 100 nm was deposited at 775 °C in 0.14 mbar of O_2 pressure using a laser energy density of 1.7 J/cm^2. Finally, 150 nm thick SBT thin films were grown with the substrate temperature and oxygen chamber pressure fixed at 740 °C and 0.2 mbar, respectively. All layers were deposited in the same chamber by changing the targets without breaking the vacuum. After the SBT film deposition, the samples were cooled to room temperature in 0.4 mbar of oxygen to prevent bismuth loss in the SBT film. Detailed deposition conditions are summarized in Table 1. Crystallographic orientations and epitaxial relations were characterized by X-ray diffraction (XRD) θ-2θ scans and pole figure measurements using a Philips X'Pert MRD 4-circle diffractometer. Cu K_α radiation and a parallel plate collimator in front of the detector with a 2θ resolution of 0.1° were used. The pole figures were measured using an open Eulerian cradle.

2 Results and discussion

Figure 1 shows the result of an XRD $\theta - 2\theta$ scan of a SBT/$SrRuO_3$/YSZ/Si structure. The figure represents well-defined (116)-oriented SBT, (110)-oriented $SrRuO_3$, and (100)-oriented YSZ films. All the Miller indices for the $SrRuO_3$ referred to in this work are based on the pseudocubic lattice parameter $a_c = 0.393$ nm [11]. For SBT an orthorhombic unit cell was assumed: $a = 0.531$ nm, $b = 0.534$ nm, and $c = 2.498$ nm [21]. The epitaxial relationship between the thin films and substrate, based on the XRD θ-2θ result, is SBT(116)‖$SrRuO_3$(110)‖YSZ(100)‖Si(100). The full-width at half maximum (FWHM) values of the SBT(22$\underline{12}$), $SrRuO_3$(110), and YSZ(200) peaks are 1.7°, 0.96°, and 1.07°, respectively, in a rocking curve θ-scan, as shown in the inset of Fig. 1. These rocking curve θ-scans suggest that YSZ is a good template layer for $SrRuO_3$ growth. One can also see an unidentified peak with low diffraction intensity of about 4% of that of the SBT(22$\underline{12}$) at $2\theta = 49.05°$. This unidentified peak belongs to a well-oriented plane, because the peak has a FWHM of $\Delta\theta = 2.2°$ in the rocking curve measurement.

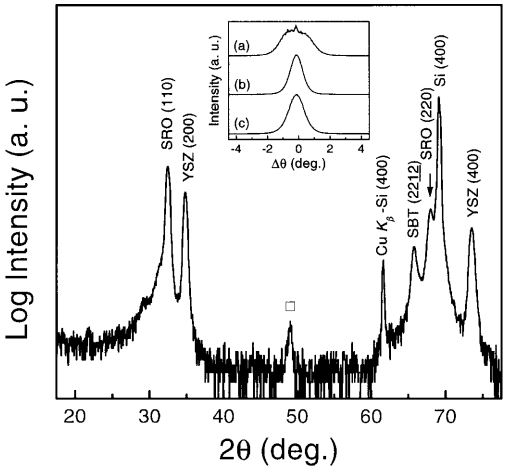

Fig. 1. X-ray θ-2θ diffraction pattern of a SBT/$SrRuO_3$/YSZ/Si structure. The SBT, $SrRuO_3$, and YSZ layers were deposited at 740 °C, 775 °C, and 800 °C, respectively. The $SrRuO_3$ peaks are indexed by pseudocubic Miller indices using the lattice parameter of $a_c = 0.393$ nm. SRO stands for $SrRuO_3$. The peak labeled as (□) is an unidentified phase. The *inset* shows θ-scans for the (a) SBT(22$\underline{12}$), (b) $SrRuO_3$(110), and (c) YSZ(200) peaks

Various pole figure analyses were conducted to confirm the crystallographic orientation and to determine whether the SBT/$SrRuO_3$/YSZ heterostructure is epitaxial. Figure 2 shows pole figures of the SBT, $SrRuO_3$, and YSZ thin films. The fixed 2θ angles used to record the pole figures in Fig. 2 are 28.97°, 25.13°, 46.18°, and 30.08° corresponding to the SBT{115}, SBT{113}, $SrRuO_3${200}, and YSZ{111} planes, respectively. The pole figures were plotted with the pole distance angle $\psi = 0°$ (center) to $\psi = 90°$ (rim). First of all, in the case of YSZ{111} in Fig. 2a, four diffraction peaks with a four-fold symmetry are observed at $\psi = 54.7°$ showing that the YSZ(100) thin film has a very good in-plane orientation. The values of the tilt distribution of the YSZ(200) reflection and of the in-plane twist misalignment of the YSZ(111) reflections, measured by θ-rocking curve and ϕ-scan, were 1.07° and 1.13°, respectively; our resolution in ϕ-scan as measured on the Si(111) was 0.21°.

An apparent degeneracy with a four-fold symmetry (four-fold epitaxial positioning) of the $SrRuO_3$ thin film can be seen at $\psi = 45°$ in the pole figure of Fig. 2b. Each set shows two symmetric diffraction peaks with an offset $\Delta\phi$ of $\sim 20°$. The separation of the reflection peaks in the pole figure of Fig. 2b provides direct evidence for the specific in-plane-epitaxial growth pattern of $SrRuO_3$ on YSZ illustrated in Fig. 3. Domains of each of the four azimuthal orientation variants of the (110)-oriented $SrRuO_3$ in Fig. 3 are present in the $SrRuO_3$ thin film. These orientation variants result in the degeneracy of the pole figure (Fig. 2b), with the characteristic separation angle of 19.5°. This angle results from the azimuthal angle of 9.75° between the $SrRuO_3$[001] and YSZ[010] directions, as indicated in Fig. 3. From this schematic dia-

Table 1. Growth conditions for SBT, $SrRuO_3$, and YSZ thin films by PLD

	SBT	$SrRuO_3$	YSZ
Target	$SrBi_{2.6}Ta_2O_9$	$SrRuO_3$	$ZrO_2 + 10$ mol %Y_2O_3
Substrate temperature (°C)	740	775	800
Oxygen pressure (mbar)	0.20	0.14	0.17×10^{-2}
Laser pulse energy density (J/cm^2)	3.4	1.7	1.7

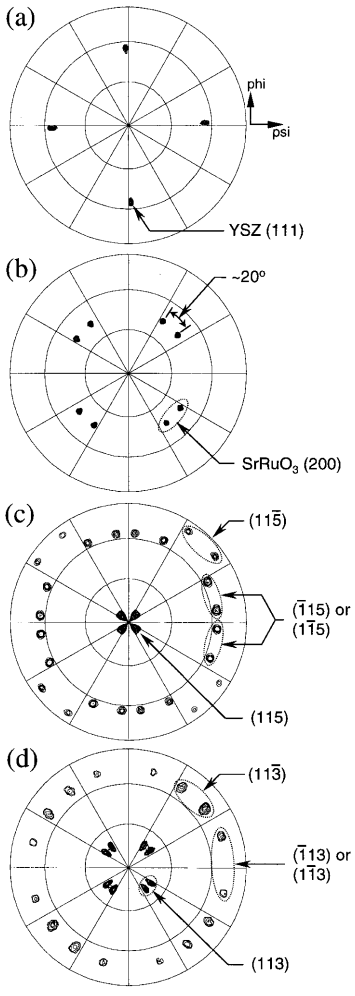

Fig. 2a–d. X-ray pole figures of a SBT/$SrRuO_3$/YSZ/Si heterostructure: **a** YSZ{111}, **b** $SrRuO_3${200}, **c** SBT{115}, and **d** SBT{113}. The fixed 2θ angles were 30.08°, 46.18°, 28.97°, and 25.13°, respectively

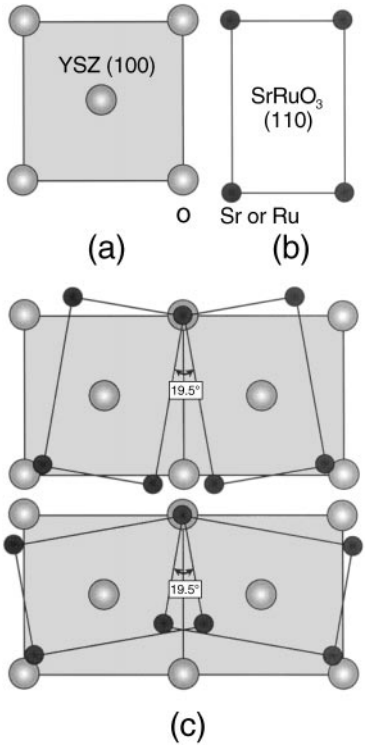

Fig. 3a–c. Schematic drawing of the rectangle-on-cube epitaxy of $SrRuO_3$ on YSZ: **a** (100) plane of YSZ, **b** (110) plane of $SrRuO_3$, and **c** four variants of the epitaxial rectangle-on-cube relationship of $SrRuO_3$ on YSZ

gram and the X-ray diffraction results, the epitaxial orientation relationship of the $SrRuO_3$ thin film on YSZ/Si(100) can be described as $SrRuO_3$(110)‖YSZ(100)‖Si(100) and $SrRuO_3$[111]‖YSZ[110]‖Si[110] taking into account that the $SrRuO_3$[111] direction may be parallel to any of the four YSZ directions [110], [$\bar{1}$10], [1$\bar{1}$0], and [$\bar{1}\bar{1}$0]. However, despite the high intensity of the $SrRuO_3$(110) diffraction peak in the θ-2θ scan of Fig. 1, relatively broad peaks with a FWHM of 2.94° were found in the ϕ-scan, which is comparably higher than that of the YSZ(111) with a value of 1.13°. Obviously, such a relatively broad distribution originates from the large lattice mismatch of −6.3% between the interplanar spacings of $SrRuO_3$(111) and YSZ(110). A similar growth trend of $SrRuO_3$(110) thin films on YSZ(100)/Si(100) substrates had been observed before [22].

In order to analyze the in-plane orientation of the SBT thin film, two pole figure measurements were performed at $2\theta = 28.97°$ and $2\theta = 25.13°$ for the SBT{115} and {113} planes, respectively (Fig. 2c and d). In Fig. 2c, the innermost four peaks centered at $\psi = 5.2°$ originate from the SBT(115) plane, which is the plane of the strongest diffraction intensity. From this pole figure, it is concluded that the SBT(116) plane is parallel to the substrate surface, because the angle between the (116) and (115) planes of SBT is 5.16°. Moreover, the diffraction peaks from ($\bar{1}$15) or (1$\bar{1}$5), and (11$\bar{5}$) are also present in Fig. 2c at $\psi = 65.1°$ and $\psi = 81.3°$. Although a pole figure of {115} peaks is sufficient to identify the orientation, we further examined the sample by taking one more pole figure of SBT{113} to unambiguously confirm the epitaxial orientation as shown in Fig. 2d. In this figure, we can clearly observe the peaks from (113), (11$\bar{3}$), and ($\bar{1}$13) or (1$\bar{1}$3) at $\psi = 18.1°$, 68.4°, and 73.1°, respectively. As expected from both the pole figure in Fig. 2b and the schematic drawing of a rectangle-on-cube epitaxy of $SrRuO_3$ in Fig. 3, all SBT peaks have a fourfold degeneracy having two symmetric peaks with an offset, $\Delta\phi$, of ∼ 20°. By referring to the pole figures, the epitaxial relationship between SBT and $SrRuO_3$ can be given as SBT(116)‖$SrRuO_3$(110); SBT[110]‖$SrRuO_3$[001] (orthorhombic indexing of SBT). A similar epitaxial relationship between SBT(106) and the titanate $SrTiO_3$(110) was already reported as SBT[010]‖$SrTiO_3$[001] (tetragonal indexing of SBT) [23]. In the latter article, the authors, however, used a tetragonal indexing of SBT with $a \approx b \approx 0.39$ nm. Further work to evaluate the ferroelectric and dielectric properties and the microstructure of the SBT(116) thin films is under way.

3 Conclusions

We have grown non-c-oriented epitaxial SBT thin films on Si substrates with $SrRuO_3$ and YSZ buffer layers. A rectangle-on-cube type of epitaxy between $SrRuO_3$ and YSZ revealed that $SrRuO_3$ and YSZ are good template layers including a bottom electrode for the growth of (116)-oriented SBT thin

films on Si(100) substrates. The epitaxial relationship determined by X-ray diffraction is SBT(116)‖$SrRuO_3$(110)‖YSZ (100)‖Si(100); SBT[110]‖$SrRuO_3$[001].

Note added in proof

Meanwhile, ferroelectric hysteresis loops of the (116-oriented SBT films on $SrRuO_3$ bottom electrodes on YSZ-buffered Si(100) have been recorded, giving a remanent polarization $P_r = 3.4\,\mu C/cm^2$ and a coercive field $E_c = 71\,kV/cm$ at a maximum applied electric field of $283\,kV/cm$.

References

1. See, for example, Abstracts of 12th International Symposium on Integrated Ferroelectrics, Aachen, Germany, 12–15 March, 2000
2. A. Gruverman: Appl. Phys. Lett. **75**, 1452 (1999)
3. A. Gruverman, A. Pignolet, K.M. Satyalakshmi, M. Alexe, N.D. Zakharov, D. Hesse: Appl. Phys. Lett. **76**, 106 (2000)
4. M. Alexe, C. Harnagea, D. Hesse, U. Gösele: Appl. Phys. Lett. **75**, 1793 (1999)
5. J.F. Scott: Abstracts of 12th International Symposium on Integrated Ferroelectrics, Aachen, Germany, 12–15 March, 2000, p. 102
6. J. Lettieri, Y. Jia, M. Urbanik, C.I. Weber, J-P. Maria, D.G. Schlom, H. Li, R. Ramesh, R. Uecker, P. Reiche: Appl. Phys. Lett. **73**, 2923 (1998)
7. K. Ishikawa, H. Funakubo: Appl. Phys. Lett. **75**, 1970 (1999)
8. S.E. Moon, T.K. Song, S.B. Back, S.-I. Kwun, J.-G. Yoon, J.S. Lee: Appl. Phys. Lett. **75**, 2827 (1999)
9. A. Pignolet, C. Schäfer, K.M. Satyalakshmi, C. Harnagea, D. Hesse, U. Gösele: Appl. Phys. **A70**, 283 (2000)
10. Y. Shimakawa, Y. Kubo, Y. Nakagawa, T. Kamiyama, H. Asano, F. Izumi: Appl. Phys. Lett. **74**, 1904 (1999)
11. C.B. Eom, R.J. Cava, R.M. Fleming, J.M. Phillips, R.B. van Dover, J.H. Marshall, J.W.P. Hsu, J.J. Krajewski, W.F. Peck, Jr.: Science **258**, 1766 (1992)
12. C.L. Chen, Y. Cao, Z.J. Huang, Q.D. Jiang, Z. Zhang, Y.Y. Sun, W.N. Kang, L.M. Dezaneti, W.K. Chu, C.W. Chu: Appl. Phys, Lett. **71**, 1047 (1997)
13. N.D. Zakharov, K.M. Satyalakshmi, G. Koren, D. Hesse: J. Mater. Res. **14**, 4385 (1999)
14. M.A. Zurbuchen, J. Lettieri, S.K. Streiffer, Y. Jia, M.E. Hawley, A.H. Carim, D.G. Schlom: Abstracts of 12th International Symposium on Integrated Ferroelectrics, Aachen, Germany, 12–15 March, 2000, p. 51
15. K. Saito, T. Akai, T. Suzuki, Y. Nishi, M. Fujimoto, A. Sakai: Abstracts of 12th International Symposium on Integrated Ferroelectrics, Aachen, Germany, 12–15 March, 2000, p. 71
16. A. Pignolet, C. Harnagea, A.R. James, D. Hesse, U. Gösele: Abstracts of 12th International Symposium on Integrated Ferroelectrics, Aachen, Germany, 12–15 March, 2000, p. 111
17. J. Lettieri, M.A. Zurbuchen, Y. Jia, D.G. Schlom, S.K. Streiffer, M.E. Hawley: Appl. Phys. Lett. **76**, 2937 (2000)
18. A. Pignolet, C. Curran, M. Alexe, S. Senz, D. Hesse, U. Gösele: Integr. Ferroelectr. **21**, 485 (1998)
19. D.K. Fork, D.B. Fenner, G.A.N. Connell, J.M. Phillips, T.H. Geballe: Appl. Phys. Lett. **57**, 1137 (1990)
20. Q.X. Jia, X.D. Wu, D.S. Zhou, S.R. Foltyn, R. Tiwari, D.E. Peterson, T.E. Mitchell: Philos. Mag. Lett. **72**, 385 (1995)
21. A.D. Rae, J.G. Thompson, R.L. Withers: Acta Cryst. **B48**, 418 (1992)
22. See, for instance, S.Y. Hou, J. Kwo, R.K. Watts, J.Y. Cheng, D.K. Fork: Appl. Phys. Lett. **67**, 1387 (1995)
23. T. Nagahama, T. Manabe, I. Yamaguchi, T. Kumagai, T. Tsuchiya, S. Mizuta: Thin Solid Films **353**, 52 (1999)